A Control Study of a Kneeless Biped Locomotion System

by JIANN-SHIOU YANG

Department of Computer Engineering, University of Minnesota, Duluth, MN 55812, U.S.A.

ABSTRACT: *In this paper, a control study on a three-degree-of-freedom kneeless biped locomotion system is performed. Based on the biped dynamics and joint trajectories of the walking gait, a robust adaptive control scheme consisting of a control law and an adaptation law was used. The control law has the structure of the inverse dynamics servo but uses estimates of the dynamics parameters in the computation of torques which propel the biped. The adaptation law uses the tracking error to compute the parameter estimates for the control law. To improve the convergence of the estimated parameters, we modify the timing of applying the adaptation by incorporating a dead zone operation. Our simulation results show that the adaptive control technique can be effectively used for the biped locomotion control. The joint tracking errors can be made acceptably small and the performance is also robust despite relatively large deviations in the initial estimates of the system parameters.*

I. Introduction

In recent years, many studies have been done in the area of legged locomotion. Efforts are being made to develop quadruped/hexapod locomotion robots for use under extreme environments such as in nuclear power plants and on ocean floors. However, research on biped locomotion has been making slow progress, mainly because of control difficulty with stable biped locomotion as compared with multi-legged locomotion. Studies about dynamic biped locomotion can be roughly classified into two main classes according to their aims. The first one aims to discover walking characteristics by measuring the human motions during locomotion. The second one aims at analyzing biped locomotion from the viewpoint of torque control at each joint. The latter class, which is mainly investigated by engineering oriented groups, is very important in finding the control law of human walking and in deriving the control algorithms of biped locomotion machines. Research on bipeds was inspired by the wish to build aids for the disabled and to understand human locomotion for scientific and medical reasons.

The major problem associated with the analysis and control of biped locomotion systems is the high-order, highly coupled nonlinear dynamics due to the multiple degrees of freedom which are inherent to the structure. The complexity makes the synthesis of a control law difficult to be realized by the direct application of modern control theory. Therefore, proper control strategies which make use of the characteristics of biped locomotion should be developed.

0016-0032(94)E0002-Z

The inverse dynamics (or computed torque) control is a well known technique for the robot motion control (**1–3**). Practical implementation of the control scheme requires that the parameters in the dynamic model of the system be known precisely. However, in any physical system there is a degree of uncertainty regarding the values of various parameters. The method may perform poorly due to inexact cancellation of the nonlinearities between the modeled dynamics and actual system dynamics. Although several adaptive inverse dynamics based control methods have been successfully used to control the robot motion (**3–7**), the success of using them for bipeds has not been reported yet. The difficulty of using such robot control techniques for biped locomotion is that we need to deal with different sets of nonlinear dynamic equations for different phases, and the duration for each phase is usually very short. The number of parameters to be estimated is also large for even a relatively simple biped system. Therefore, it will be interesting to investigate whether the adaptive inverse dynamics based control methods can still be effectively used for the biped locomotion control. The paper will focus on this study. We consider a three-degree-of-freedom biped locomotion system. Based on the dynamics of the walking gait and joint trajectories, a standard adaptive inverse dynamics control scheme consisting of a control law and an adaptation law is applied. The control law has the structure of the inverse dynamics servo but uses estimates of the dynamics parameters in the computation of torques which propel the biped. The adaptation law uses the tracking error to compute the parameter estimates for the control law, stops updating a given parameter when it reaches its known bounds, and resumes updating as soon as the corresponding derivative changes sign. We conducted extensive computer simulations to evaluate the biped locomotion control. Our results show that the tracking errors can be improved with the parameters associated with the adaptation law properly chosen, and the performance is also robust despite relatively large deviations in the initial parameter estimates. We also found that several existing robot control techniques (**6–8**) cannot be applied to the biped locomotion control.

The paper is organized as follows. In Section II, we briefly review the adaptive control method. The descriptions of the biped system is then given in Section III. In Section IV, we discuss the implementation aspects of the control scheme and then present our simulation results. Finally, Section V gives some concluding remarks.

II. The Adaptive Inverse Dynamics Control

Since linearized system equations cannot always be trusted to accurately predict the responses of real (nonlinear) systems, we directly consider nonlinear control and briefly review the adaptive control scheme (**1**, **2**) to be used in our biped locomotion system.

A standard method for deriving the dynamic equations of mechanical systems is via the Lagrange's formulation [see (**9**) for details]. Using this method the equations of motion of an n-link rigid robot can be written as

$$D(q)\ddot{q}+C(q,\dot{q})\dot{q}+g(q) = \tau, \tag{1}$$

where q is the $n \times 1$ vector of joint displacements, τ is the $n \times 1$ vector of applied joint torques (or forces), $D(q)$ is the $n \times n$ symmetric positive definite inertia matrix, $C(q, \dot{q})\dot{q}$ is the $n \times 1$ vector of centripetal and Coriolis torques, and $g(q)$ is the $n \times 1$ vector of gravitational torques. By the property of *linearity in the parameters*, the dynamic equations can be writen as

$$D(q)\ddot{q} + C(q, \dot{q})\dot{q} + g(q) = Y(q, \dot{q}, \ddot{q})p, \tag{2}$$

where $Y(q, \dot{q}, \ddot{q})$ is an $n \times r$ matrix of known functions, known as the regressor, and p is an r-dimensional vector of parameters (**1–7, 9**).

Inspecting (1) we see that if the control τ is chosen as

$$\tau = D(q)a + C(q, \dot{q})\dot{q} + g(q), \tag{3}$$

then, by substituting (3) into (1) and using the property of $D(q)$ one obtains

$$\ddot{q} = a. \tag{4}$$

The vector term a can be defined in terms of a given linear compensator $K(s)$ as

$$a = \ddot{q}^d - K(s)e \tag{5}$$

with $e = q - q^d$, where $q^d(t)$ is an n-dimensional vector of desired joint trajectories. Substituting (5) into (4) leads to the linear error equation

$$[s^2 I_n + K(s)]e = 0 \tag{6}$$

where I_n is an $n \times n$ identity matrix. Letting $K(s) = K_v s + K_p$ leads to the familiar second-order error equation

$$\ddot{e} + K_v \dot{e} + K_p e = 0. \tag{7}$$

If the gain matrices K_v and K_p are chosen as diagonal matrices with positive diagonal elements then the closed-loop system is linear, decoupled and exponentially stable.

The above approach is based on exact cancellation of all nonlinearities in the system. However, in any physical system there is a degree of uncertainty regarding the values of various parameters. There will always be inexact cancellation of the nonlinearities in the system due to this uncertainty and also due to computational round-off, etc. In addition, the burden of computing the complete model may be prohibitively expensive or impossible within the bounds imposed by the available computer architecture. In such cases it is desirable to simplify the equations of motion as much as possible by ignoring certain of the terms in the equations in order to speed the computation of the control law. Therefore, it is much more reasonable to suppose that, instead of (3), the nonlinear control law is actually of the form

$$\begin{aligned} \tau &= \hat{D}(q)a + \hat{C}(q, \dot{q})\dot{q} + \hat{g}(q), \\ a &= \ddot{q}^d - K_v \dot{e} - K_p e, \end{aligned} \tag{8}$$

where $\hat{D}$, $\hat{C}$ and $\hat{g}$ are the estimates of D, C and g, respectively. Assume that $\hat{D}$, $\hat{C}$ and $\hat{g}$ have the same functional form as D, C, g with estimated parameters $\hat{p}_1, \hat{p}_2, \ldots, \hat{p}_r$, then

Vol. 331B, No. 2, pp. 125–143, 1994

$$\hat{D}(q)\ddot{q}+\hat{C}(q,\dot{q})\dot{q}+\hat{g}(q) = Y(q,\dot{q},\ddot{q})\hat{p} \tag{9}$$

where $\hat{p} = [\hat{p}_1, \hat{p}_2, \ldots, \hat{p}_r]^T$ is the vector of the estimated parameters and the superscript T means the transpose.

Substituting (8) into (1) gives

$$D\ddot{q}+C\dot{q}+g = \hat{D}(\ddot{q}^d - K_v\dot{e} - K_p e)+\hat{C}\dot{q}+\hat{g}. \tag{10}$$

Adding and subtracting $\hat{D}\ddot{q}$ on the left-hand side of (10) and using (9), we get

$$\hat{D}(\ddot{e}+K_v\dot{e}+K_p e) = \tilde{D}\ddot{q}+\tilde{C}\dot{q}+\tilde{g} = Y(q,\dot{q},\ddot{q})\tilde{p} \tag{11}$$

where $\tilde{(\cdot)} := \hat{(\cdot)} - (\cdot)$. Finally the error dynamics may be written as

$$\ddot{e}+K_v\dot{e}+K_p e = \hat{D}^{-1}Y\tilde{p} := \Phi\tilde{p}. \tag{12}$$

The system (12) can be expressed in state space as

$$\dot{x} = Ax+B\Phi\tilde{p} \tag{13}$$

where

$$A = \begin{pmatrix} 0 & I_n \\ -K_p & -K_v \end{pmatrix}; \quad \text{and} \quad B = \begin{pmatrix} 0 \\ I_n \end{pmatrix}; \quad x = \begin{pmatrix} e \\ \dot{e} \end{pmatrix}. \tag{14}$$

Based on (13) and (14), we choose the update law

$$\dot{\hat{p}} = -\Gamma^{-1}\Phi^T B^T P x \tag{15}$$

where $\Gamma = \Gamma^T > 0$ and P is the unique symmetric positive definite solution to the Lyapunov equation

$$A^T P + PA = -Q \tag{16}$$

for a given symmetric, positive definite Q. Since the parameter vector p is constant, $\dot{\tilde{p}} = \dot{\hat{p}}$. Assuming that $\ddot{q}$ is measurable and $\hat{D}^{-1}$ is bounded, then the solution x of (13) satisfies $x \to 0$ as $t \to \infty$ with all signals remaining bounded [for proof, see (**1**, **2**)]. The adaptive control scheme is shown in Fig. 1.

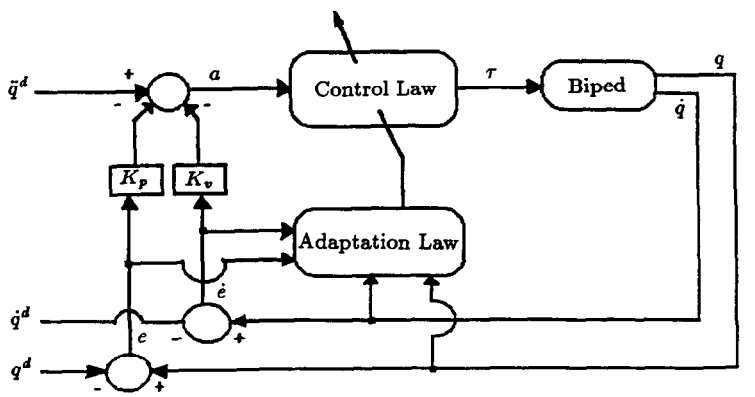

FIG. 1. The adaptive inverse dynamics control scheme.

There are several different versions of (**1**, **2**). For example, the boundedness of the estimated inertia $\hat{D}^{-1}$ is removed in (**4**), while in (**5**) the requirement on measurement of $\ddot{q}$ is removed but one still needs the boundedness of $\hat{D}^{-1}$. Several recent papers have been devoted to the implementation of the above adaptive inverse dynamics method without measuring $\ddot{q}$. Most of the results amount, in one guise or another, to estimating $\ddot{q}$ from $\dot{q}$ using a first-order filter. In practice, this approach should be expected to work well.

III. The Biped Dynamical System

The major problem associated with the analysis and control of biped locomotion systems is the high-order, highly coupled nonlinear dynamics due to the multiple degrees of freedom which are inherent to the structure. Hence, to study the dynamics of legged locomotion systems, it becomes imperative to select mechanical models having few degrees of freedom to keep the equations of motion to a manageable level, yet having enough degrees of freedom to accurately represent the motion involved.

In this paper, we study the walking gait control of a simplified three-degree-of-freedom kneeless biped moving in a sagittal plane as shown in Fig. 2(a), where θ_i $(i = 1, 2, 3)$ are the joint angles, (x_h, y_h) represents the hip coordinates, and the function $g_s(x)$ defines the terrain surface. Forces acting on the system are the gravitational forces and the hip actuator torques M_2 (right leg) and M_4 (left leg). There are no frictional forces at the hip joints. Strictly speaking, the model shown in Fig. 2(a) cannot achieve locomotion due to foot–ground collisions during walking. The free-swinging leg would always scrape the ground when brought forward. Since the purpose of this paper is to study the feasibility of applying the control scheme in Fig. 1 to a biped locomotion system, the knee joints were intentionally eliminated in order to handle a system having only three degrees of freedom. Although the feet have been eliminated from the biped model, the actions of the feet and the manner in which they generate the ankle actuator torques (M_1 for the right leg and M_3 for the left leg) on the model will be considered. In other words, to control the biped, torques are assumed to be present at all joints including the base (ankle) of the leg supporting the biped. The parameters of mass (m_i), center of mass location (c.m.), and the moment of inertia (I_i) about c.m. for each segment are defined in Fig. 2(b). The parameter values are taken from (**10**, **11**) which are close to those of the legs and trunk of the average human male. That is, $m_1 = m_3 = 12.2$ kg, $m_2 = 49.0$ kg, $l_{a1} = l_{a3} = 0.387$ m, $l_{b1} = l_{b3} = 0.546$ m, $l_2 = 0.280$ m, $I_1 = I_3 = 0.697$ kg m^2 and $I_2 = 2.35$ kg m^2. Only the control of walking gait on a level surface is considered. Control of the biped motion in a three-dimensional space is more complicated. A prospective method is to decompose the biped motion into the sagittal plane component and the lateral plane component, and to control each motion component with synchronized support leg exchange.

Observation of a normal human walk reveals that each gait cycle of the biped can be divided into four distinct phases: (a) right leg support phase; (b) right leg to left leg support exchange phase; (c) left leg support phase; and (d) left leg to right leg support exchange phase. Therefore, the equations of motion describing

Vol. 331B, No. 2, pp. 125–143, 1994

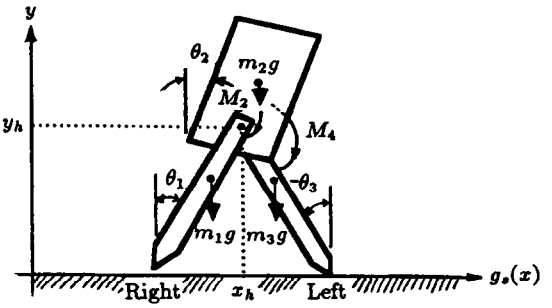

(a)

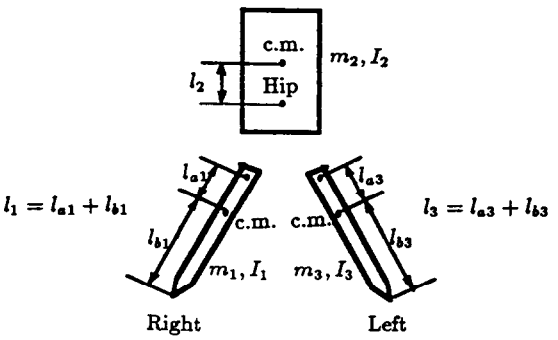

(b)

FIG. 2. A three-degree-of-freedom kneeless biped.

the dynamics of the biped walking gait consists of four sets of equations, one for each support phase. The equations of motion can be obtained by using the Lagrange's method to derive the equations of the biped in a free-fall configuration (i.e. no feet constraints applied), and then impose the desired constraints on these equations to obtain the equations of motion for each of the support phases. For simplicity, assume that the terrain surface is rigid and has an infinite coefficient of friction (i.e. no sinking or slipping occurs) and the duty cycle of the double leg support phases can be neglected, i.e. the biped instantaneously exchanges support from one leg to the other. From Fig. 2(a), the constraints for the feet of the biped are:

(i) right leg support phase: $t_{2i} < t < t_{2i+1}$, $i = 0, 1, 2, \ldots$

$$x_h - l_1 \sin \theta_1 = s_{2i},$$
$$y_h - l_1 \cos \theta_1 = g_s(s_{2i}); \tag{17}$$

(ii) left leg support phase: $t_{2i+1} < t < t_{2i+2}$, $i = 0, 1, 2, \ldots$

$$x_h - l_3 \sin\theta_3 = s_{2i+1},$$
$$y_h - l_3 \cos\theta_3 = g_s(s_{2i+1}), \tag{18}$$

where the s_i ($i = 0, 1, \ldots$) are the x-coordinates of the support points on the terrain surface and the t_i are the times when the biped instantly exchanges support from one leg to the other.

By Lagrange's formulation, the dynamics of one complete cycle of the walking gait of the kneeless biped can be found as follows [for derivations, see (**10**)]:

(i) right leg support phase: $t_{2i} < t < t_{2i+1}$

$$\ddot{\theta}_1 + \alpha_{r12}[\ddot{\theta}_2 \cos(\theta_1 - \theta_2) + \dot{\theta}_2^2 \sin(\theta_1 - \theta_2)] - \alpha_{r13}[\ddot{\theta}_3 \cos(\theta_1 - \theta_3) + \dot{\theta}_3^2 \sin(\theta_1 - \theta_3)] - \beta_{r1} \sin\theta_1 = \gamma_{r1}(M_1 - M_2),$$
$$\ddot{\theta}_2 + \alpha_{r2}[\ddot{\theta}_1 \cos(\theta_2 - \theta_1) + \dot{\theta}_1^2 \sin(\theta_2 - \theta_1)] - \beta_{r2} \sin\theta_2 = \gamma_{r2}(M_2 + M_4),$$
$$\ddot{\theta}_3 - \alpha_{r3}[\ddot{\theta}_1 \cos(\theta_3 - \theta_1) + \dot{\theta}_1^2 \sin(\theta_3 - \theta_1)] + \beta_{r3} \sin\theta_3 = -\gamma_{r3} M_4; \tag{19}$$

(ii) right leg to left leg support exchange: $t = t_{2i+1}$

$$\dot{\theta}_1^+ + \varepsilon_{l1}\dot{\theta}_1^- - \alpha_{l1}\dot{\theta}_3^+ \cos(\theta_1 - \theta_3) = 0,$$
$$\dot{\theta}_2^+ - \dot{\theta}_2^- + \alpha_{l2}\dot{\theta}_3^+ \cos(\theta_2 - \theta_3) - \alpha_{r2}\dot{\theta}_1^- \cos(\theta_2 - \theta_1) = 0,$$
$$\dot{\theta}_3^+ + \varepsilon_{l33}\dot{\theta}_3^- + \alpha_{l32}(\dot{\theta}_2^+ - \dot{\theta}_2^-)\cos(\theta_3 - \theta_2) - (\alpha_{l31}\dot{\theta}_1^+ + \varepsilon_{l31}\dot{\theta}_1^-)\cos(\theta_3 - \theta_1) = 0; \tag{20}$$

(iii) left leg support phase: $t_{2i+1} < t < t_{2i+2}$

$$\ddot{\theta}_1 - \alpha_{l1}[\ddot{\theta}_3 \cos(\theta_1 - \theta_3) + \dot{\theta}_3^2 \sin(\theta_1 - \theta_3)] + \beta_{l1} \sin\theta_1 = -\gamma_{l1} M_2,$$
$$\ddot{\theta}_2 + \alpha_{l2}[\ddot{\theta}_3 \cos(\theta_2 - \theta_3) + \dot{\theta}_3^2 \sin(\theta_2 - \theta_3)] - \beta_{l2} \sin\theta_2 = \gamma_{l2}(M_2 + M_4),$$
$$\ddot{\theta}_3 + \alpha_{l32}[\ddot{\theta}_2 \cos(\theta_3 - \theta_2) + \dot{\theta}_2^2 \sin(\theta_3 - \theta_2)] - \alpha_{l31}[\ddot{\theta}_1 \cos(\theta_3 - \theta_1) + \dot{\theta}_1^2 \sin(\theta_3 - \theta_1)] - \beta_{l3} \sin\theta_3 = \gamma_{l3}(M_3 - M_4); \tag{21}$$

(iv) left leg to right leg support exchange: $t = t_{2i+2}$

$$\dot{\theta}_1^+ + \varepsilon_{r11}\dot{\theta}_1^- + \alpha_{r12}(\dot{\theta}_2^+ - \dot{\theta}_2^-)\cos(\theta_1 - \theta_2) - (\alpha_{r13}\dot{\theta}_3^+ + \varepsilon_{r13}\dot{\theta}_3^-)\cos(\theta_1 - \theta_3) = 0,$$
$$\dot{\theta}_2^+ - \dot{\theta}_2^- + \alpha_{r2}\dot{\theta}_1^+ \cos(\theta_2 - \theta_1) - \alpha_{l2}\dot{\theta}_3^- \cos(\theta_2 - \theta_3) = 0,$$
$$\dot{\theta}_3^+ + \varepsilon_{r3}\dot{\theta}_3^- - \alpha_{r3}\dot{\theta}_1^+ \cos(\theta_3 - \theta_1) = 0. \tag{22}$$

The α, β, γ and ε coefficients are functions of the masses, inertia and length parameters (**10**) and $\dot{\theta}^+ = \dot{\theta}(t_i^+)$, $\dot{\theta}^- = \dot{\theta}(t_i^-)$ in (ii) and (iv). Note that in a free-fall configuration, the biped has five degrees of freedom; however, the application of the two foot constraints has eliminated two degrees of freedom (i.e. x_h and y_h). Also, the discontinuity occurs in $\dot{\theta}$ during the leg support exchange.

By recording the motion of the lights (e.g. light-emitting diodes) attached to the links of a biped, which is moved through the locomotion cycle of positions, the

trajectories for the joint angles that produce a walking gait can be found. Observations of normal human walking gaits show that the average gait velocity $v = 0.853$ m s^{-1} and the gait stride length $l_s = 0.546$ m (**12**). Using these values for the kneeless biped, the periodic response of the walking gait for one cycle is:

(i) right leg support phase: $0 < t < T$

$$\theta_1(t) = 0.264 \sinh(3.08t - 1.02) + 0.037\theta_3(t),$$
$$\theta_2(t) = 0,$$
$$\theta_3(t) = -0.368 \sin(6.52t - 2.16); \tag{23}$$

(ii) left leg support phase: $T < t < 2T$

$$\theta_1(t) = -0.368 \sin(6.52(t - T) - 2.16),$$
$$\theta_2(t) = 0,$$
$$\theta_3(t) = 0.264 \sinh(3.08(t - T) - 1.02) + 0.037\theta_1(t); \tag{24}$$

where $T = l_s/v$ ($= 0.64$ s) is the period of a single leg support phase and $2T$ is the period of a gait cycle. The desired joint trajectories are shown in Fig. 3.

IV. Simulation Results

Based on the desired trajectories and biped dynamics, the control scheme described in Section II will be used to control the biped motion.

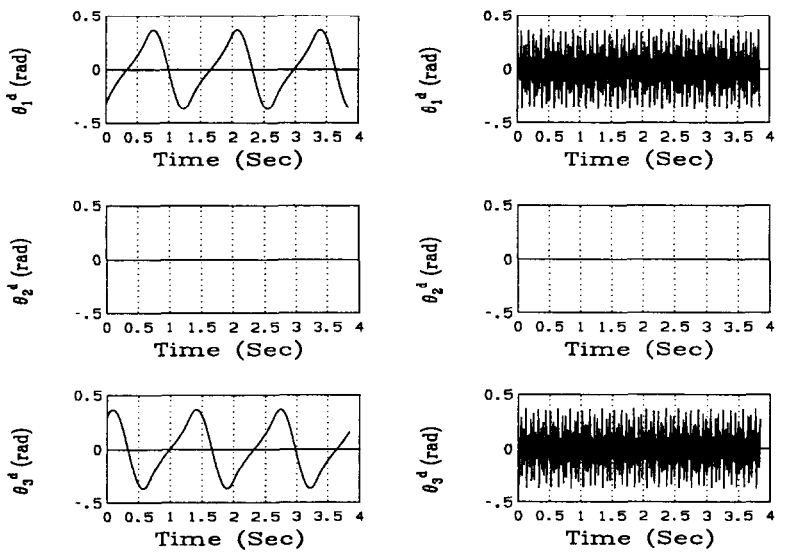

FIG. 3. Desired joint trajectories: (a) three complete cycles; (b) 100 complete cycles.

4.1. *Implementation aspects*

Let $\tau = [M_1 - M_2, M_2 + M_4, M_4]^T$ and $\tau = [M_2, M_2 + M_4, M_3 - M_4]^T$ be the torques in (1) for the right leg and left leg support phases, respectively. Using (2) and the dynamical equation sets (19) and (21), the regressor $Y(\theta, \dot{\theta}, \ddot{\theta})$ with $\theta = [\theta_1, \theta_2, \theta_3]^T$ will be a 3×10 matrix. Therefore, in the implementation of the adaptation law (15) there are 10 parameters to be estimated for each leg support phase, i.e. P_{ri}† and P_{li}‡ $(i = 0, 1, \ldots, 9)$ for the right and left leg support phases, respectively. Using the nominal parameter values given in Section II, we choose $K_v = 6.325 I_3$, $K_p = 10.0 I_3$ for $K(s)$ and $Q = 10^4 I_6$.

Note that the adaptation law uses the tracking error to compute the parameter estimates for the control law, stops updating a given parameter when it reaches its known bounds, and resumes updating as soon as the corresponding derivative changes sign. Due to the short duration of the support phases for each cycle, the parameters do not have the time required to converge within one cycle. Therefore, the parameter estimates must be carried between cycles to allow for convergence. However, from simulations we found that the parameters still showed no signs of converging. This is due to the transitions which occurred at the time of support phase transfers. To overcome this problem, the adaptation incorporated with a dead zone of 0.2 s is introduced immediately after the phase change occurs, i.e. during the first 0.2 s of each support and free swing phases, no adaptation occurred and after that, adaptation resumes.

4.2. *Computer simulations*

In order to study the robustness of the adaptive control scheme, we let masses m_i vary one at a time by $\pm 25\%$ of their nominal values and then compare the performance with and without adaptation. The total duration time we considered is 100 cycles (i.e. 128 s). The control torques are generated from (8) based on the parameter estimates from (15) where the inverse of the adaptation gain matrix, i.e. Γ^{-1} is properly assigned. Figure 4 shows the joint tracking errors (in radians) with and without adaptation under the torso's weight -25% variations, i.e. we reduce the torso's weight from its nominal value 49.0 kg to 36.75 kg. The desired joint trajectories θ_1^d and θ_3^d lie between ± 0.4 radians while θ_2^d is zero. From Fig. 4(a), we see that without adaptation the errors are unacceptably large (i.e. ~ -0.2 radians for e_1, e_3 and $+0.5$ radians for e_2). However, after applying adaptation with $\Gamma^{-1} = 0.14 I_{10}$, the performance has been dramatically improved and the joint errors become negligibly small [see Fig. 4(b)]. The torque waveforms τ_i $(i = 1, 2, 3)$ are shown in Fig. 5 where we found that their magnitudes are within the ranges in rough agreement with the magnitudes of walking humans calculated by other

† $P_{r0} = m_1 l_{a1}^2 + I_1 - 2m_1 l_1 l_{a1} + (m_1 + m_2 + m_3) l_1^2$, $P_{r1} = \alpha_{r12}/\gamma_{r1} = m_2 l_1 l_2$, $P_{r2} = \alpha_{r13}/\gamma_{r1} = m_3 l_1 l_{a3}$, $P_{r3} = (m_1 + m_2 + m_3) l_1 g - m_1 l_{a1} g$, $P_{r4} = m_2 l_2^2 + I_2$, $P_{r5} = \alpha_{r2}/\gamma_{r2} = m_2 l_1 l_2$, $P_{r6} = m_2 l_2 g$, $P_{r7} = m_3 l_{a3}^2 + I_3$, $P_{r8} = \alpha_{r3}/\gamma_{r3} = m_3 l_1 l_{a3}$ and $P_{r9} = m_3 l_{a3} g$.

‡ $P_{l0} = m_1 l_{a1}^2 + I_1$, $P_{l1} = \alpha_{l1}/\gamma_{l1} = m_1 l_3 l_{a1}$, $P_{l2} = m_1 l_{a1} g$, $P_{l3} = m_2 l_2^2 + I_2$, $P_{l4} = m_2 l_3 l_2$, $P_{l5} = m_2 l_2 g$, $P_{l6} = \alpha_{l31}/\gamma_{l3} = m_1 l_3 l_{a1}$, $P_{l7} = m_2 l_3 l_2$, $P_{l8} = m_3 l_{a3}^2 + I_3 - 2m_3 l_3 l_{a3} + (m_1 + m_2 + m_3) l_3^2$ and $P_{l9} = (m_1 + m_2 + m_3) l_3 g - m_3 l_{a3} g$.

Vol. 331B, No. 2, pp. 125–143, 1994

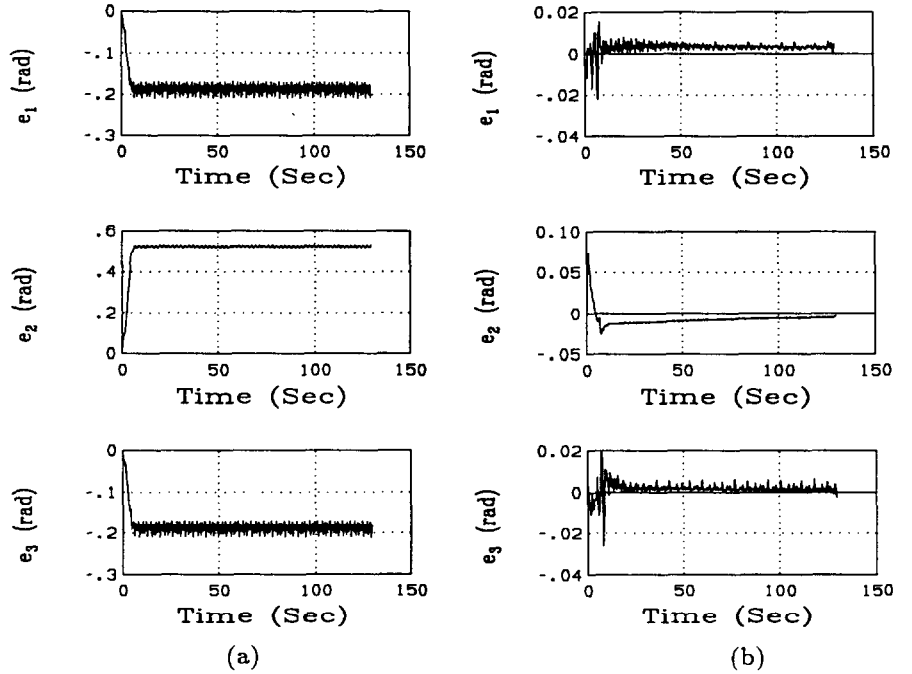

FIG. 4. Position errors under the torso's weight −25% variations. (a) Without adaptation; (b) with adaptation.

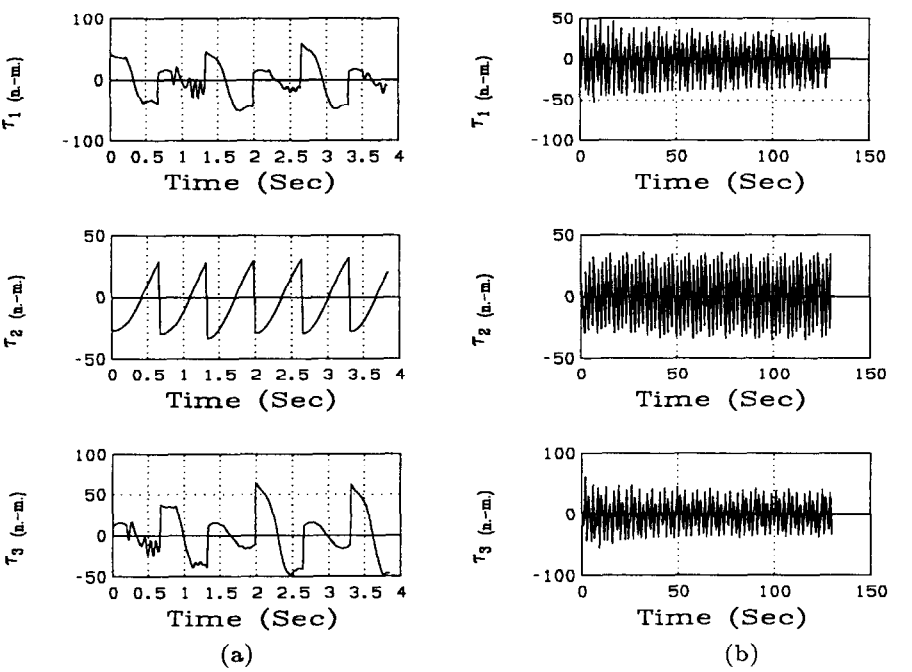

FIG. 5. Torque τ_i $(i = 1, 2, 3)$ time responses. (a) Three complete cycles; (b) 100 complete cycles.

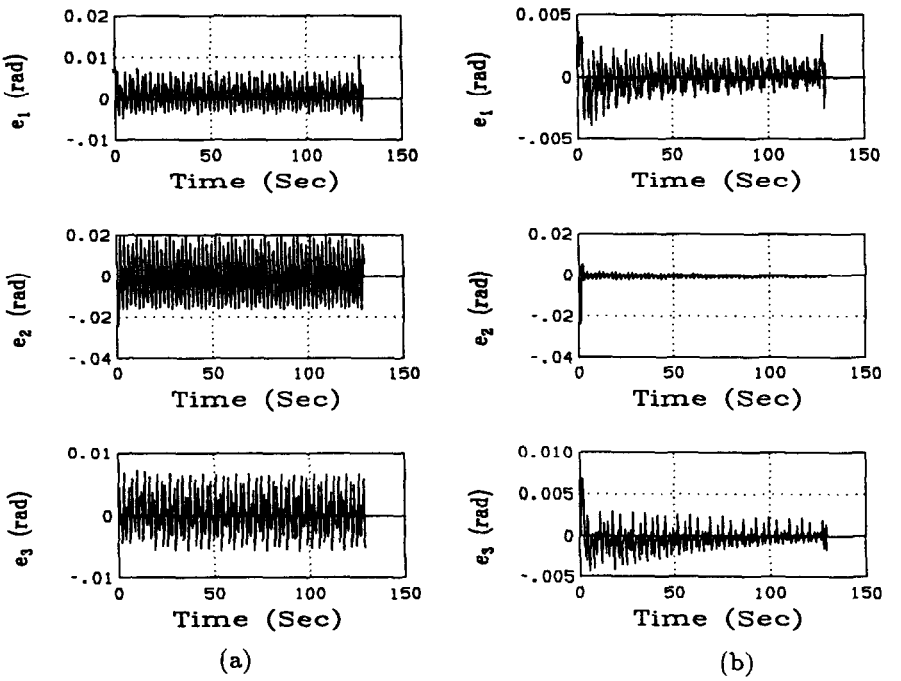

FIG. 6. Position errors under the torso's weight +25% variations. (a) Without adaptation; (b) with adaptation.

methods (**13, 14**). The error responses under the torso's weight +25% increase are shown in Fig. 6, and as we can see the performance has also been improved when the adaptation with $\Gamma^{-1} = 0.05I_{10}$ was applied. The corresponding torque responses τ_i under the adaptation are given in Fig. 7. Note that increasing the torso's weight has less effect on the tracking errors as compared with that of decreasing the weight. The time evolution of the estimated parameters (i.e. the vector $\hat{p}$) for the right and left leg support phases for the case of Fig. 4 is shown in Figs 8 and 9, respectively. From Figs 8 and 9, we see that most of these 20 parameters appear to converge or come close to converging to a constant value although the values that the parameters converge to are not equal to their true values. Note that by using the adaptive control scheme, tracking can be achieved without the estimated parameters converging to their true values. It is known that in order for the parameter estimates to converge to their true values, the reference trajectory must be "sufficiently rich", i.e. the trajectory must sufficiently excite the dynamics of the system so that the effects of the various parameters can be distinguished. For the control scheme given in Section II, parameter convergence is attained if $B^{\mathrm{T}}P(sI-A)^{-1}B$ is strictly positive real and the regressor $Y(q^d, \dot{q}^d, \ddot{q}^d)$ is persistently exciting (**2, 3**). The joint errors by varying the mass m_3 by $\pm 25\%$ are given in Figs

Vol. 331B, No. 2, pp. 125–143, 1994

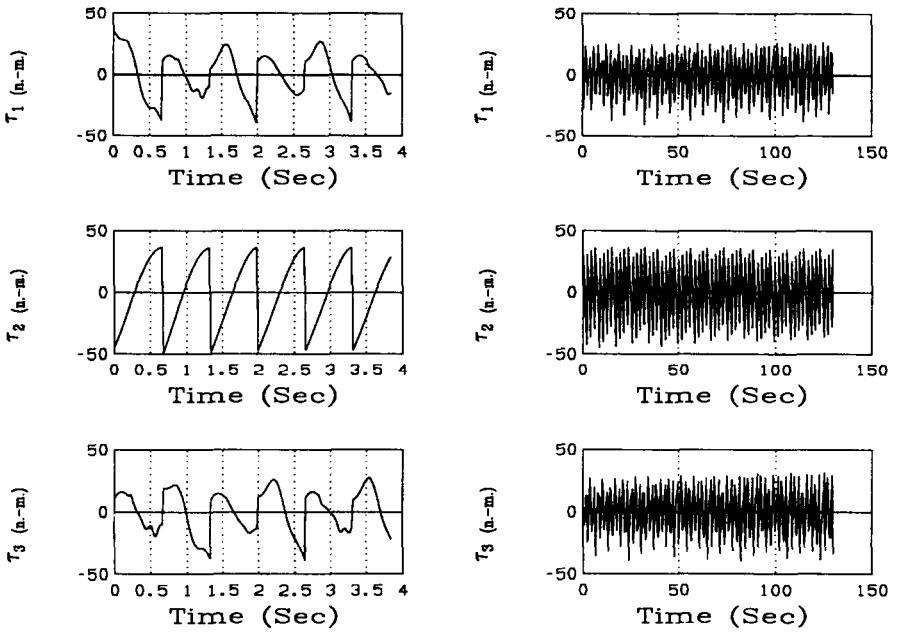

FIG. 7. Torque τ_i $(i = 1, 2, 3)$ time responses. (a) Three complete cycles; (b) 100 complete cycles.

10 and 11, respectively. From these figures, we see that the performance has been improved after the adaptation with $\Gamma^{-1} = 0.13I_{10}$ and $\Gamma^{-1} = 0.05I_{10}$ were applied, respectively. We found very similar results by perturbing the weight m_1.

The error performance under m_1, m_2 and m_3 simultaneous $\pm 25\%$ variations was also studied, and the results are shown in Figs 12 and 13. It is interesting to note that decreasing m_i $(i = 1, 2, 3)$ by 25% causes the tracking errors very similar to that of decreasing m_2 only (see Fig. 4). As expected, the overall performance was improved with $\Gamma^{-1} = 0.12I_{10}$ and $\Gamma^{-1} = 0.10I_{10}$ for the cases of Figs 12 and 13, respectively. The torque responses we found also lie within the same ranges as those given in Figs 5 and 7. The comparison of simultaneous parameter changes with different amounts of variations from their nominal values in the initial setting was also studied. We found that the errors and duration time for (parameter) convergence appear to be less for the small deviations in the initial estimates. The values that the parameters converge to are not equal for different cases, nor are they equal to their nominal values.

In order to test the robustness to an external disturbance acting at the joints, the process noise was added in the form of random perturbations at the torque outputs of the actuators. The results under $m_2 \pm 25\%$ variations are shown in Figs 14 and

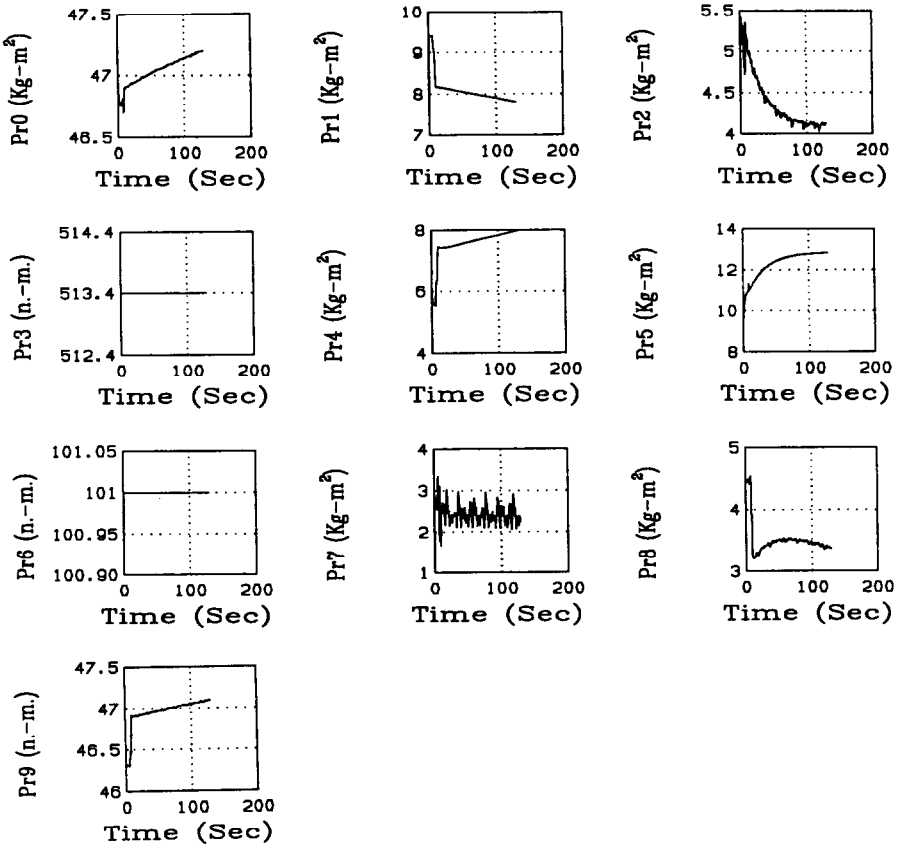

FIG. 8. Parameter estimates for the right leg support phase for the first 100 cycles.

15, which are the same as that of Figs 4 and 6 except that a substantial amount of noise has been added to the torque at each joint. The value of the noise amplitude lies between $\pm 10\%$ of the maximum value that can be reached by θ_1^d and θ_3^d (the desired joint trajectories). Comparing with the results of Figs 4 and 6, we see that the performance appears quite robust to such disturbances. We also found similar results by perturbing m_1 and m_3 with random noise added at the joint torques.

In (**10, 11**), Golliday considered the linearization of the equations (19)–(22) with respect to the operating point $\theta_i = \dot{\theta}_i = 0$ $(i = 1, 2, 3)$ which represents the upright standstill position of the biped, and then used the state feedback to design the locomotion control. Such a local linearization to serve as approximate representation of the nonlinear dynamics of the biped will only be valid in a very narrow region around the operating point. Therefore, it is not very effective to use the linear state feedback to control the biped walking as can be easily seen after a comparison of their results with ours. For instance, the errors generated in (**11**) without mass

Vol. 331B, No. 2, pp. 125–143, 1994

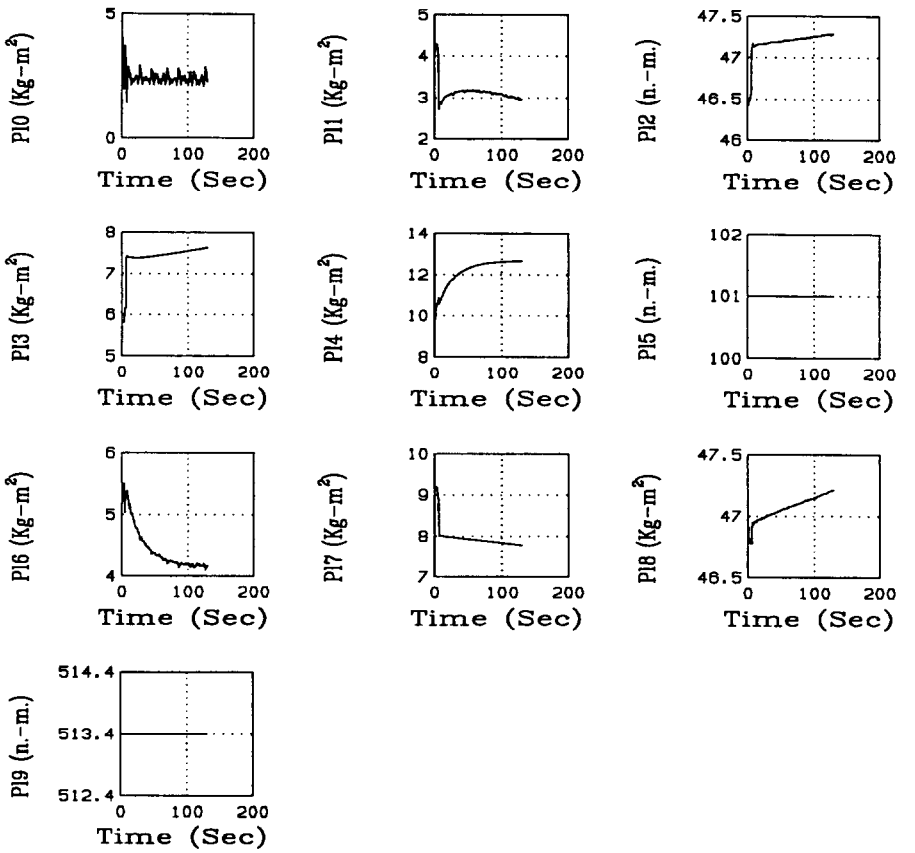

FIG. 9. Parameter estimates for the left leg support phase for the first 100 cycles.

perturbations are even larger than that of ours where the individual and simultaneous variations of the masses by $\pm 25\%$ were considered.

V. Conclusions

We have successfully applied the proposed robust adaptive control method to the biped locomotion system. The implementation of the control scheme consists of a control law and an adaptation law. The control law has the structure of the inverse dynamics servo but uses estimates of the dynamics parameters in the computation of torques which propel the biped. The adaptation law uses the tracking error to compute the parameter estimates for the control law. Simulation results show that the tracking errors are acceptably small and the performance is also robust despite relatively large deviations from the nominal values in the initial estimates of the parameters.

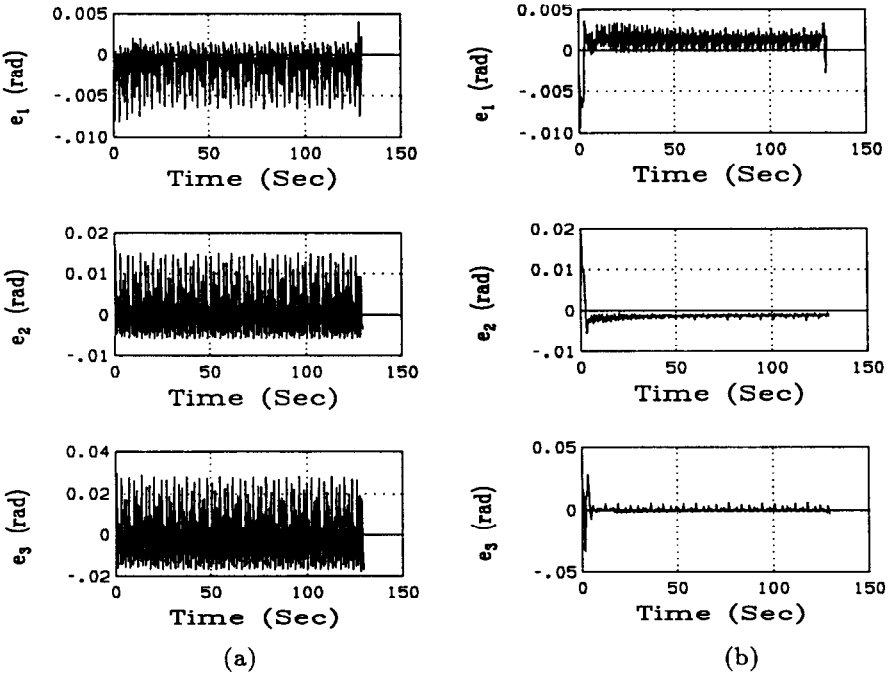

FIG. 10. Position errors under m_3 −25% variations. (a) Without adaptation; (b) with adaptation.

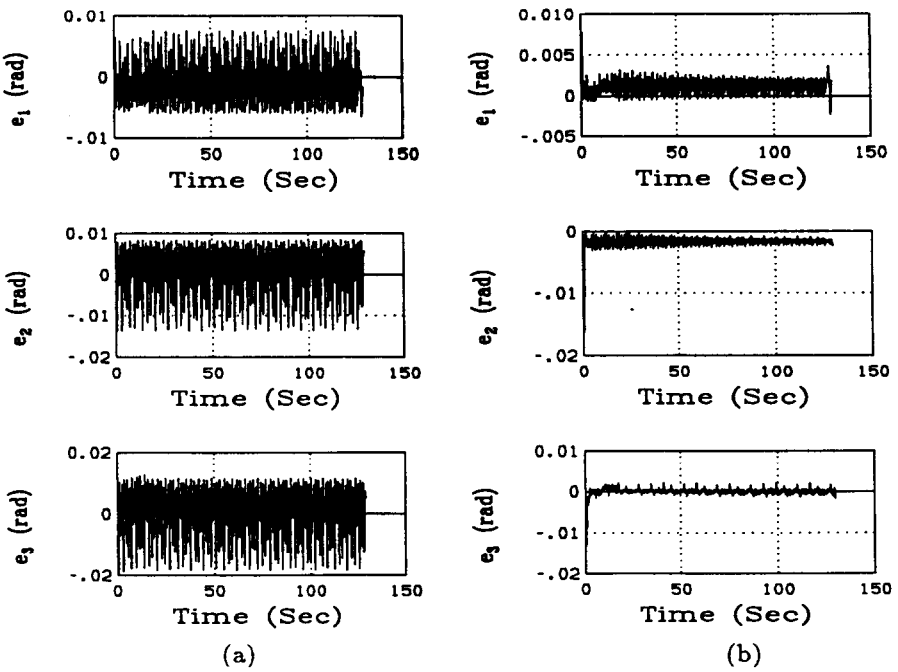

FIG. 11. Position errors under m_3 +25% variations. (a) Without adaptation; (b) with adaptation.

Vol. 331B, No. 2, pp. 125–143, 1994

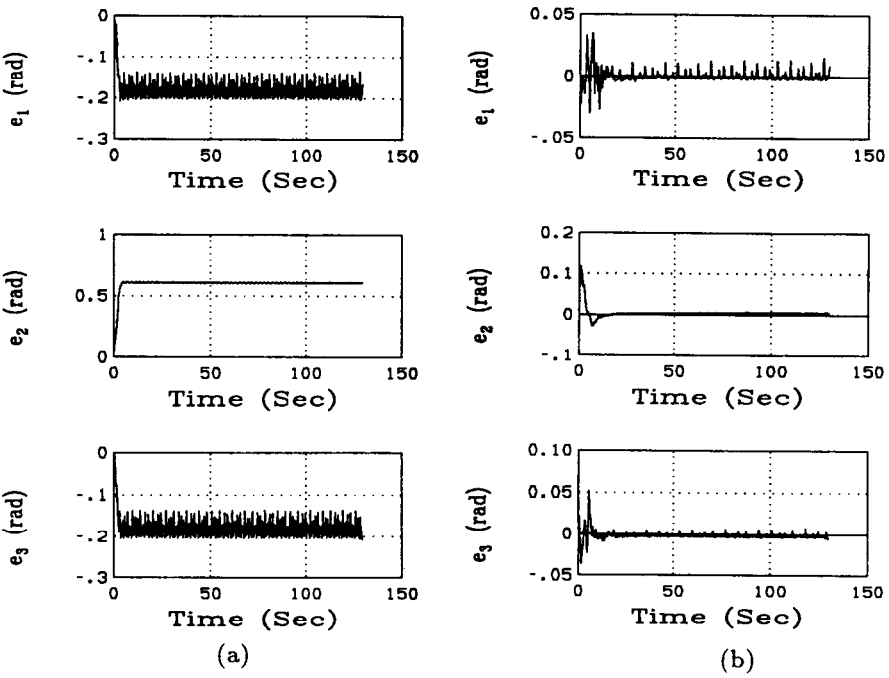

FIG. 12. Position errors with masses simultaneous −25% variations. (a) Without adaptation; (b) with adaptation.

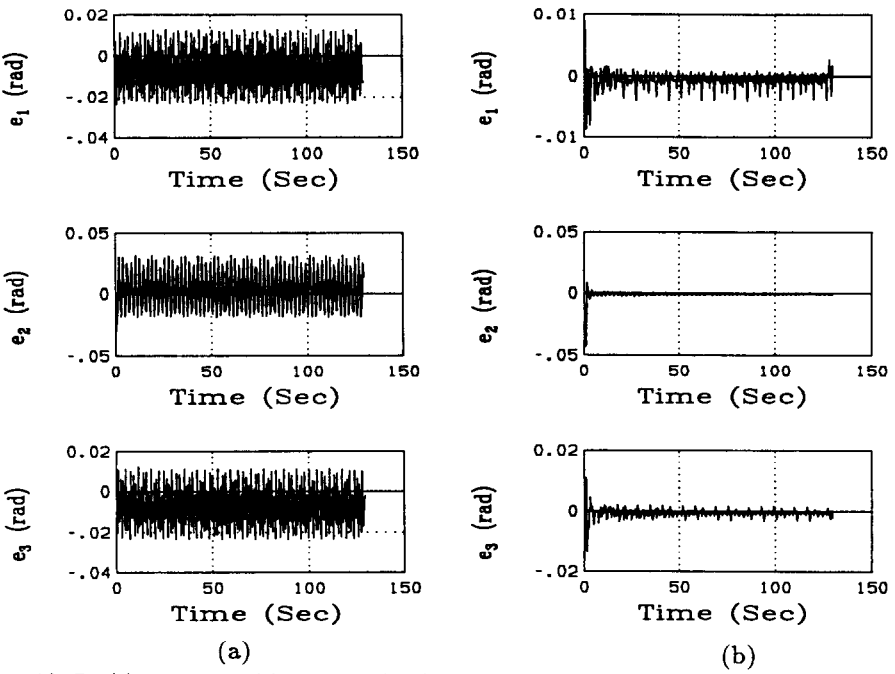

FIG. 13. Position errors with masses simultaneous +25% variations. (a) Without adaptation; (b) with adaptation.

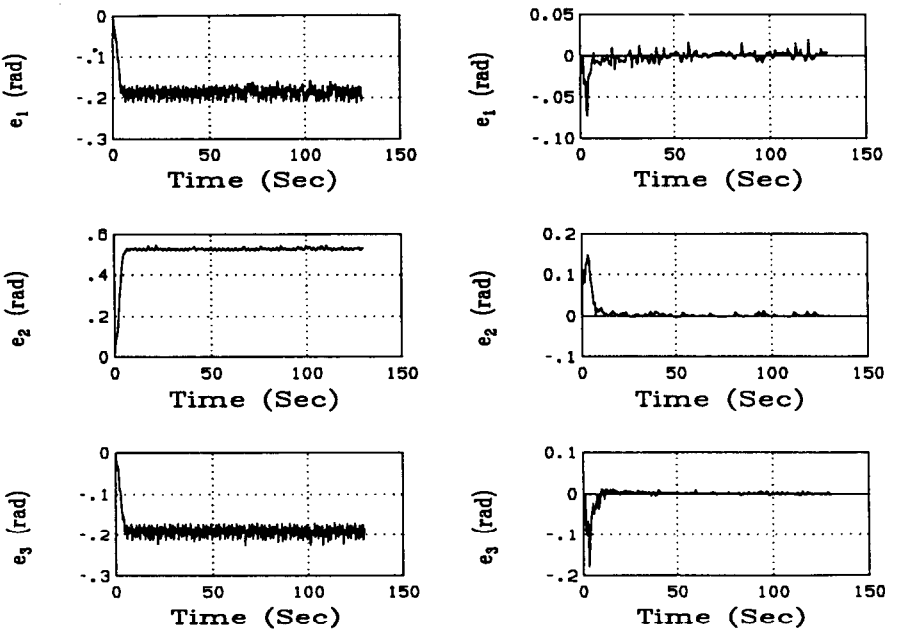

FIG. 14. Position errors under $m_2 - 25\%$ variations with random noise added. (a) Without adaptation; (b) with adaptation.

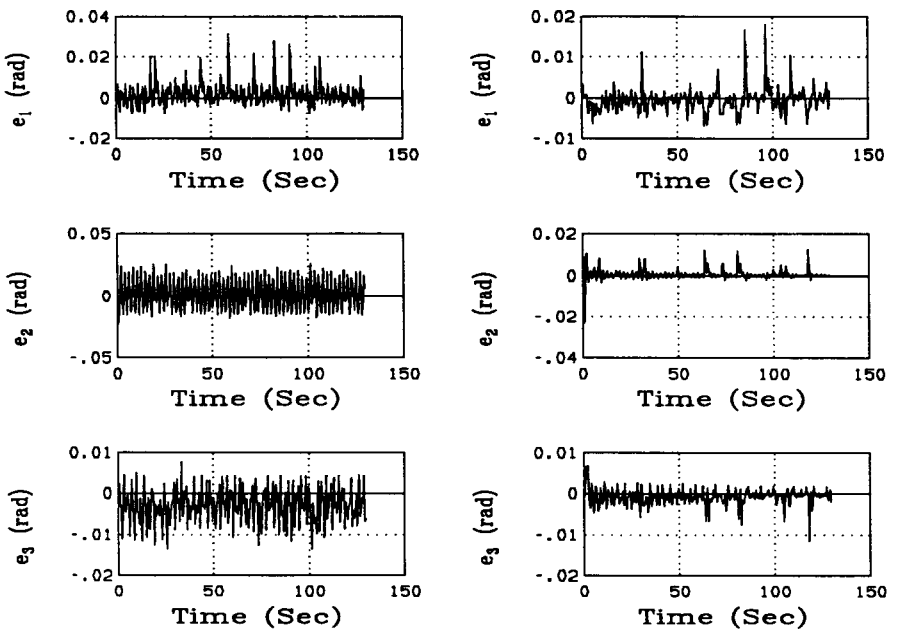

FIG. 15. Position errors under $m_2 + 25\%$ variations with random noise added. (a) Without adaptation; (b) with adaptation.

The advantage of using the inverse dynamics control method is that it formulates a globally convergent adaptive controller which does not require approximations such as local linearization, time-invariant, or decoupled dynamics to guarantee the tracking convergence. The method requires the inversion of the estimated inertia matrix and numerical differentiation of the joint velocities in order to obtain estimates of the joint accelerations. However, these can be overcome by using a modified version of the proposed method such as (**4**, **5**, **15**). To increase computational efficiency in the implementation of the proposed method, the matrices $\hat{D}$, $\hat{C}$, $\hat{g}$, and the regressor $Y(q, \dot{q}, \ddot{q})$, may be updated at a slower rate, since (1), typically the tracking error terms vary much faster than the dynamic coefficient matrices; and (2), the choice of the adaptation gain matrix Γ is generally such that the adaptation process is slower than the control bandwidth. During the simulation run, we didn't encounter the problems of non-existence and non-boundedness of $\hat{D}^{-1}$. However, we do find that some of the existing robot adaptive control techniques (**6**–**8**) fail when they are applied to the biped locomotion systems. This is because these so-called passivity-based control methods require the skew symmetry property which doesn't hold for the biped dynamics.

Acknowledgements

The research was supported in part by the Graduate School of the University of Minnesota, Minneapolis Grant-in-Aid Award No. 15324. The author wishes to thank Ahmed Shahabuddin for his assistance with the simulations.

References

(**1**) J. J. Craig, P. Hsu and S. Sastry, "Adaptive control of mechanical manipulators", "Proc. IEEE Int. Conf. on Robotics and Automation", pp. 190–195, San Francisco, CA, 1986.

(**2**) J. J. Craig, "Adaptive Control of Mechanical Manipulators", Addison-Wesley, Reading, MA, 1988.

(**3**) R. Ortega and M. W. Spong, "Adaptive motion control of rigid robots: a tutorial", *Automatica*, Vol. 25, pp. 877–888, 1989.

(**4**) M. W. Spong and R. Ortega, "On adaptive inverse dynamics control of rigid robots", *IEEE Trans. Autom. Control*, Vol. 35, pp. 92–95, 1990.

(**5**) R. H. Middleton and G. C. Goodwin, "Adaptive computed torque control for rigid link manipulators", *Systems Control Lett.*, Vol. 10, pp. 9–16, 1988.

(**6**) J.-J. E. Slotine and W. Li, "On the adaptive control of robot manipulators", *Int. J. Robotics Res.*, Vol. 6, pp. 49–59, 1987.

(**7**) R. Kelly and R. Carelli, "Input–output analysis of an adaptive computed torque plus compensation control for manipulators", "Proc. IEEE Conf. on Decision and Control", Austin, TX, 1988.

(**8**) J.-J. E. Slotine and W. Li, "Adaptive manipulator control: a case study", *IEEE Trans. Autom. Control*, Vol. 33, pp. 995–1003, 1988.

(**9**) M. W. Spong and M. Vidyasagar, "Robot Dynamics and Control", Wiley, New York, 1989.

(**10**) C. L. Golliday, "Toward Development of Biped Locomotion Controls: Planar Motion

Control of the Kneeless Biped Standing and Walking Gaits", Ph.D. Dissertation, The Ohio State University, Columbus, 1975.

(11) C. L. Golliday and H. Hemami, "An approach to analyzing biped locomotion dynamics and designing robot locomotion controls", *IEEE Trans. Autom. Control*, Vol. 22, pp. 963–972, 1977.

(12) I. S. Cheng, "Computer Television Analysis of Biped Locomotion", Ph.D. Dissertation, The Ohio State University, Columbus, 1974.

(13) M. A. Townsend and A. A. Seireg, "The synthesis of bipedal locomotion", *J. Biomech.*, Vol. 5, pp. 71–83, 1972.

(14) M. A. Townsend and A. A. Seireg, "Effect of model complexity and gait criteria on the synthesis of bipedal locomotion", *IEEE Trans. Biomed. Engng*, Vol. 20, pp. 433–444, 1973.

(15) M. Amestegui, R. Ortega and J. M. Ibarra, "Adaptive linearizing-decoupling robot control : a comparative study of different parameterizations", "Proc. 5th Yale Workshop on Applications of Adaptive Systems Theory", New Haven, CT, 1987.

Received : 29 June 1993
Accepted : 4 November 1993